Check for updates

Synthesis of a surface molecular imprinting polymer based on silica and its application in the identification of nitrocellulose

Yan Yang, Xiangjun Meng and Zhenggang Xiao ⓘ *

A surface molecular imprinting polymer (MIP) based on silica (SiO_2/MIP) with excellent selective identification properties towards nitrocellulose (NC) was synthesized with methylacrylic acid as a functional monomer and NC as a template molecule, through simple *in situ* polymerization. The functional groups of SiO_2/MIP were studied through Fourier transform infrared spectroscopy. The morphology, crystalline state and thermostability of SiO_2/MIP were investigated respectively by scanning electron microscopy, X-ray diffraction and thermogravimetric analysis. Binding capacity and selectivity studies of SiO_2/MIP for NC and its analogues were carried out through ultraviolet-visible spectrophotometry. The thermal analysis and study of crystalline states confirmed the successful imprinting of NC in the polymer networks. The optimized conditions were found to be a polymerization temperature of 45 °C and a functional monomer to cross-linking ratio of 1 : 3. The adsorption capacity of SiO_2/MIP was improved considerably compared with that of polymers prepared by traditional imprinting technology, with a maximum adsorption amount of 1.7 mg mg^{-1} in 2 mg ml^{-1} NC solution, compared with an adsorption capacity of about 0.5 mg mg^{-1} for a traditional MIP. According to the selectivity study, more NC was adsorbed by SiO_2/MIP than its analogues; the best adsorption capacity of SiO_2/MIP for NC was approaching 5 times that for carboxymethyl cellulose (CMC). The results show that it would be possible to apply SiO_2/MIP for the detection of NC, to give improved sensitivity in security checking and improved contaminant adsorption.

1. Introduction

Nitrocellulose (NC), a cellulose derivative, is a type of explosive material, which is the basic component of single and double base propellants.[1] It is also known as a versatile, widely used polymer with numerous civil applications, such as an additive in paints and lacquer coatings for automobile and wood furniture.[2,3] Recently, it has been applied in the fabrication of specific biosensors, especially in protein microarrays of biochips for its neutral effect on proteins and immobilization of enzymes.[4–7] Nevertheless, most of the terrorist attacks occurring worldwide involve the misuse of NC and other explosives. Further, the preparation of paints and lacquer coatings may cause environmental contamination such as water pollution. Therefore, in order to eliminate the occurrence of terrorist attacks and decrease the pollution of water, it is necessary to find valid methods to detect NC.

Many methods have been reported for the detection of NC. Gas chromatography (GC) combined with electron ionization (EI) and mass spectrometry (MS) was adopted by Chajistamatiou and Bakeas to identify NC in bulk explosives.[8] However, the

School of Chemical Engineering, Nanjing University of Science and Technology, Nanjing 210094, China. E-mail: xiaozhg@njust.edu.cn

application of this method is hindered by the voluminous expensive instruments. MacMillan and co-workers used ion chromatography to determine NC in soil.[9] They described the removal of impurities, extraction, hydrolysis and neutralization, followed by the analysis of free nitrate and nitrite through ion chromatography. Obviously, the disadvantage of this method is that it is laborious and time-consuming.

Considering the limitations of the above methods, it is necessary to enhance and improve NC detection technology, and more importantly, to develop a simple, highly-selective and widespread detection technology.[10]

As a highly selective and highly sensitive detection method for a particular analyte, molecularly imprinted technology (MIT)[11,12] has received increasing attention in recent years. Numerous papers in relation to MIT have been published, which involve extensive applied fields including biomedicine,[13–16] environmental protection, separation of substances[17] and so on. In general, the synthesis of a molecular imprinting polymer (MIP)[18–21] involves the polymerization of a functional monomer in the presence of a cross-linking agent and template molecules.[22] After the polymerization, the template molecules are removed from the polymer. As a result, the recognition sites, that are complementary to the template molecules in function and shape,[23,24] are left in the polymer, which gives the MIP its

ability to combine with a particular template molecule or its analogues efficiently and selectively.[25]

In spite of the synthesis of various imprinted materials, their commercial applications have not been put into practice yet. This results from the fact that the three-dimensional cavities in the synthesized MIP are not easily accessible to template molecules, thus leading to a poor binding capacity, slow binding kinetics and difficult template removal. To improve the traditional MIT, alternative approaches have been explored such as surface molecular imprinting,[26,27] magnetic molecular imprinting,[28,29] core–shell polymerization[30] *etc.* Surface molecularly imprinted technology (SMIT) has been applied extensively, because the generated cavities are located on the surface of the materials, which decreases the resistance to mass transfer thus facilitating the contact of the template molecules with recognition sites in the polymer matrix. As a result, SMIT overcomes the disadvantages of the traditional MIT.

In this paper, through a simple, time-saving and facile *in situ* polymerization process, a surface imprinting polymer was synthesized to selectively detect NC, while silica (SiO_2) was utilized as a core material. Inspired by the literature,[31] 3-(tri-methoxysilyl) propylmethacrylate (MPS) was used in the form of a modifier to functionalize SiO_2 powders with an acrylyl group. Thus through hydrogen bond interactions, it was easier for SiO_2 powders to combine with NC molecules. Then the effects of the polymerization temperature and proportions of functional monomer and cross-linking agent on the adsorption capacity of NC were investigated. The surface imprinting polymer based on SiO_2 (SiO_2/MIP) and surface non-imprinting polymer (SiO_2/NIP) were characterized by scanning electron microscopy (SEM), Fourier transform infrared spectroscopy (FT-IR), thermogravimetric analysis (TGA) and X-ray diffraction (XRD). By contrasting SiO_2/NIP and a traditional molecular imprinting polymer (TMIP), the adsorption capacity of the prepared SiO_2/MIP was studied through ultraviolet-visible (UV-vis) spectrophotometry. Selectivity studies were conducted through attaching the SiO_2/MIP to NC and related structural analogues. The results showed that, SiO_2/MIP could be applied practically to the highly selective and sensitive determination of NC in security checks and environmental protection.

2. Results and discussion

2.1 Preparation and detection principle of SiO_2/MIP

Fig. 1 illustrates the preparation process for poly(methylacrylic acid) (PMAA)/inorganic particle hybrid composites with highly selective properties for NC. Allowing for the scarce hydroxy groups on the surface of the purchased SiO_2, the core material SiO_2 was prepared directly based on the hydrolyzation of tetraethoxysilicane (TEOS), and silicon-hydroxyl condensation in a solution of ethanol and deionized water with ammonium hydroxide as a catalyst. In order to improve the interface properties, the silane coupling agent MPS was used to increase the surface activity of SiO_2 and more importantly to functionalize the SiO_2 particles with acrylyl groups for the follow-up experiments. Through ultrasonic dispersion of MPS-SiO_2 and NC in the presence of methylacrylic acid (MAA) and ethylene

glycol dimethacrylate (EGDMA), hydrogen bonds were formed between the ester group in MPS-SiO_2 and the hydroxy group in NC. At the same time, NC was orientated in the mixture by the formation of hydrogen bonds between its nitro group and the carboxy group in MAA. After the addition of 2,2-azobisisobutyronitrile (AIBN), a simple *in situ* polymerization took place by which NC was assembled and immobilized in the polymer network formed by MAA and EGDMA on the surface of the SiO_2 particles. Subsequently, a mixture of methanol and acetic acid was used for the removal of the template NC, owing to the stronger hydrogen bonding interactions formed among carboxy groups in acetic acid, hydroxy groups in methanol and NC, in conditions of excess methanol and acetic acid. The NC was distributed on the surface of the SiO_2 owing to its pre-combination with MPS-SiO_2, thus benefitting the final removal approach using methanol and acetic acid. After the removal of the template NC, cavities were left on the surface of SiO_2, which retained the shape, size and functional groups of NC, thus the resultant SiO_2/MIP was able to selectively identify the template NC.

TMIP was prepared without the addition of SiO_2; hydrogen bonds existed only between the hydroxy groups and nitro groups in NC and carboxy groups in MAA. In consequence, the template NC was stuck in the three-dimensional polymer networks formed after the polymerization process. When methanol and acetic acid were used to try to remove the template NC, access to the chasmal template NC was restricted which resulted in template residue in the polymer. As a result, the adsorption capacity of TMIP was poor in the rebinding test.

2.2 FT-IR analysis

Fig. 2 shows the FT-IR spectra of the prepared surface imprinting polymer based on SiO_2 particles. Fig. 2(A) shows the FT-IR measurements of (a) SiO_2 and (b) MPS-SiO_2. The characteristic absorption peaks at 3372 cm^{-1} and 946 cm^{-1} belong to the stretching vibration and bending vibration of Si–OH groups on the surface of SiO_2.[32] The peaks located at 1047 cm^{-1} and 793 cm^{-1} are assigned to Si–O–Si stretching vibrations. The peaks observed at 2920 cm^{-1} and 1700 cm^{-1} belong to the stretching vibration of –CH_3 and C=O in MPS, which indicates that the SiO_2 particles were successfully modified by MPS through a condensation reaction between hydroxy groups on the surface of SiO_2 particles and methoxy groups in MPS.

Fig. 2(B) shows the FT-IR spectra of SiO_2/MIP, SiO_2/NIP and NC. From the spectra, it can be seen that the characteristic peaks of SiO_2/MIP and SiO_2/NIP are highly consistent. The peak at 1723 cm^{-1} belongs to the stretching vibration of C=O in MAA and EGDMA. Peaks at 1458 cm^{-1}, 1388 cm^{-1} and 1141 cm^{-1} are assigned to the bending vibrations of C–H in –CH_3 and –CH_2. Peaks at 1253 cm^{-1} and 950 cm^{-1} are attributed to the C–O stretching vibration and –OH in-plane rocking vibration in the carboxy group, respectively. In the spectrum of NC, the strong absorption peaks located at 1637 cm^{-1} and 1274 cm^{-1} are assigned to the –NO_2 stretching vibration, whereas peaks at 820 cm^{-1}, 747 cm^{-1} and 677 cm^{-1} belong to the –NO_2 bending vibration.
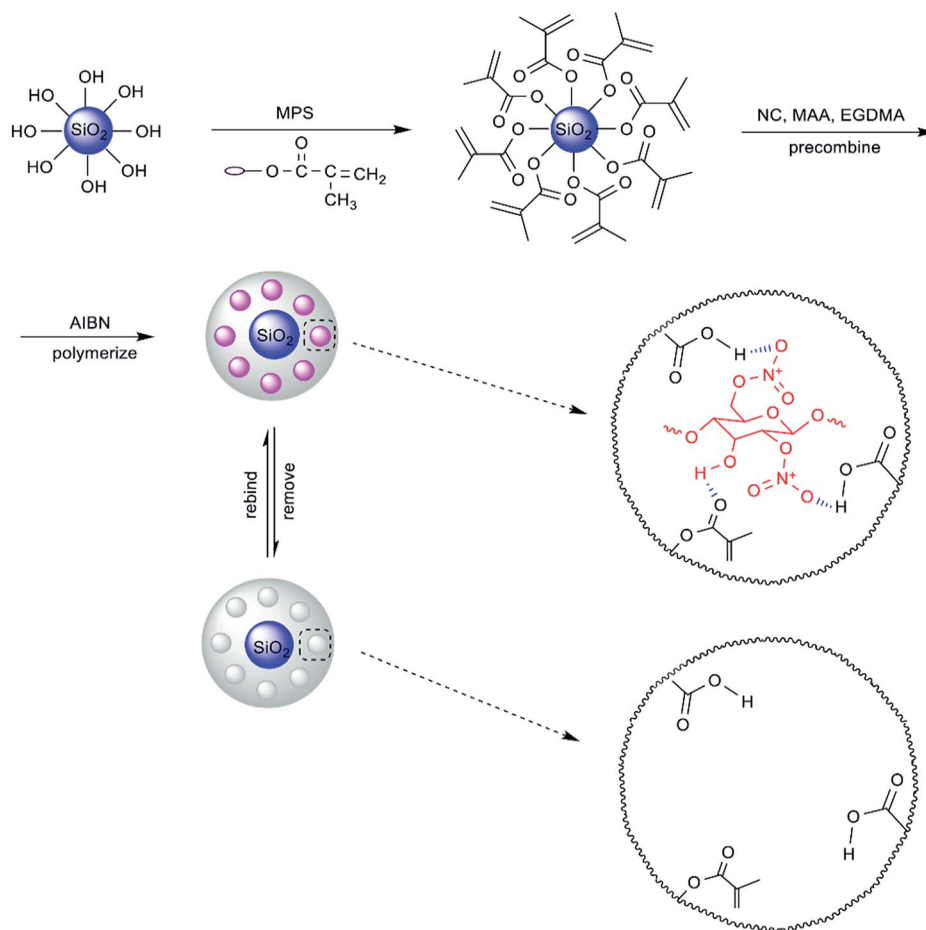
Fig. 1 Schematic diagram of the imprinting process of nitrocellulose on the surface of SiO₂.

By contrasting the spectrum of NC, it is clear that there are no remarkable absorption peaks of NC observed in the spectrum of SiO$_2$/MIP, which indicates the thorough removal of the template NC in the process of SiO$_2$/MIP synthesis. This is because the imprinting sites in the cavities in SiO$_2$/MIP are located on the surface of the SiO$_2$ particles, leading to easier access to the NC for the mixture of methanol and acetic acid. On the other hand, the imprinting sites in TMIP are embedded into the three-dimensional polymer network, which results in the difficulty for methanol and acetic acid to bind the NC molecules.

2.3 Morphological analysis

The morphologies of the synthesized SiO$_2$ were studied by SEM as presented in Fig. 3. From Fig. 3(a) and (b), the synthesized SiO$_2$ particles exhibit a spherical shape and smooth surface, while the diameter of the SiO$_2$ particles ranges from 280 nm to 585 nm. It is easy to see that the SiO$_2$ particles are stacked and agglomerated together. This behavior might be due to the high surface free energy of SiO$_2$ particles of small granularity.[33]

Fig. 4 depicts the SEM images of TMIP (a and b), TNIP (c and d), SiO$_2$/MIP (e and f) and SiO$_2$/NIP (g and h). As shown in Fig. 4(a), the polymers in the traditional MIT sample exhibit cross-linked networks in which many cavities are observed, while TNIP is observed to form many large agglomerates. With

higher magnification, the TMIP is shown to be made up of irregular spherules with many interstices (Fig. 4(b)), while the surface of TNIP is close-grained and fluctuant (Fig. 4(d)). A polyporous polymer matrix is observed in Fig. 4(e); SiO$_2$ particles appear embedded in the polymer, and some SiO$_2$ particles are on the surface of the polymer (Fig. 4(f)). In Fig. 4(g), many independent blocks are dispersed, and SiO$_2$ particles are submerged into the polymer or on the surface of the polymer (Fig. 4(h)). The SEM images of embedded SiO$_2$ particles in Fig. 4 indicate that the molecular imprinting process of SiO$_2$/MIP takes place on the surface of the SiO$_2$ particles. At the same time, some SiO$_2$ particles are not embedded in the polymer, which might due to the easy agglomeration of SiO$_2$ particles with small granularity. The carbonyl groups and hydroxyl on the surface of MPS-SiO$_2$ are occupied by other SiO$_2$ particles in the process of agglomeration. As a result, this proportion of the SiO$_2$ particles cannot contact the groups in MAA and EGDMA sufficiently. Thus in the polymerization process, it is difficult for agglomerated SiO$_2$ particles to be embedded in the polymer.

With the reported imprinting process using template NC in the synthesis of MIP, the imprinted sites complementary with NC are left in the MIP once the template is removed, leading to the polyporous structures of TMIP and SiO$_2$/MIP. On the other hand, without the NC imprinting, there are no cavities and imprinted
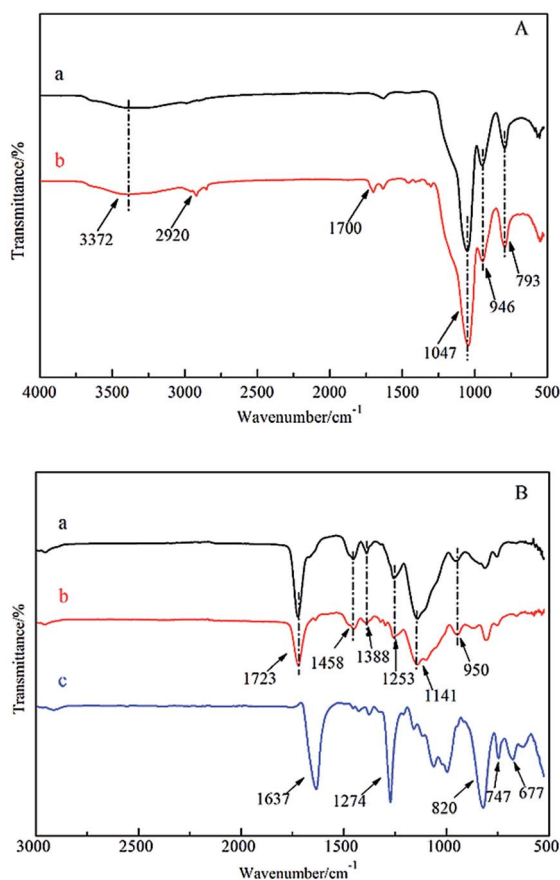
Fig. 2 FT-IR spectra of the prepared surface imprinting polymers based on silica particles: (A) (a) SiO_2, (b) MPS–SiO_2, and (B) (a) SiO_2/MIP, (b) SiO_2/NIP, (c) NC.
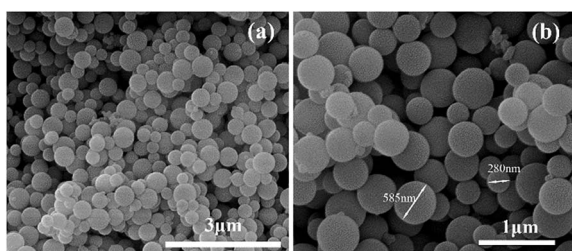

Fig. 4 SEM images of TMIP (a and b), TNIP (c and d), SiO_2/MIP (e and f), SiO_2/NIP (g and h). Magnification (a) 10000×, (b, d, f and h) 40000×, (c) 5000 ×, (e and g) 20000×.

Fig. 3 SEM images of the synthesized SiO_2 particles: magnification (a) 20000×, (b) 40000×.

sites in TNIP and SiO_2/NIP, which explains the agglomerates and blocks observed in the SEM images of TNIP and SiO_2/NIP.

2.4 XRD characterization

Fig. 5 shows the X-ray diffractograms of TMIP, TNIP, SiO_2/MIP, SiO_2/NIP and SiO_2. In the X-ray diffractogram of SiO_2 particles, the wide hump in the range of 15° to 30° is typical for amorphous silica.[34] The SiO_2/MIP does not have diffraction peaks, while peaks in SiO_2/NIP, TMIP and TNIP can be seen at an angle of 15°. Meanwhile, the intensity of the peaks decreases progressively according to the sequence of TNIP > SiO_2/NIP >
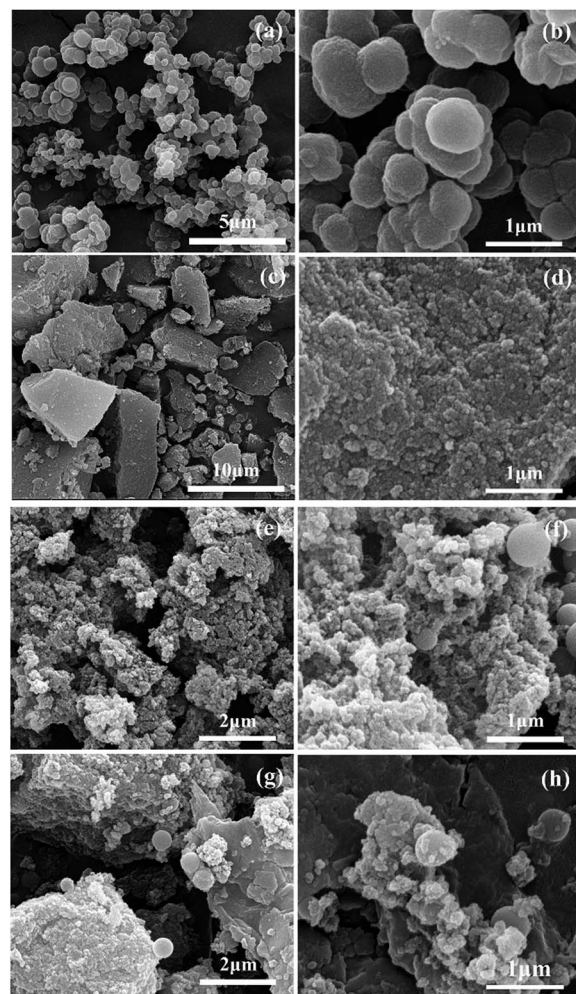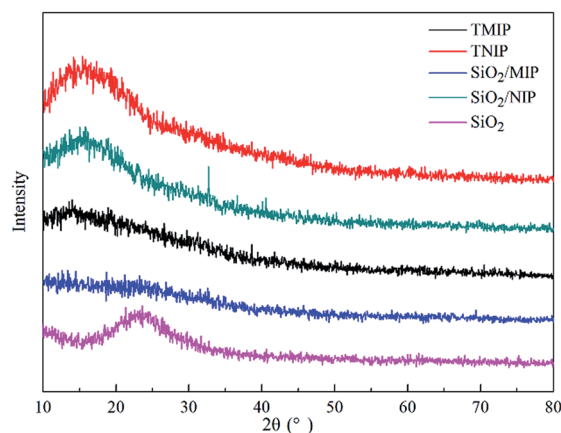

Fig. 5 X-ray diffractograms of TMIP, TNIP, SiO_2/MIP, SiO_2/NIP and SiO_2.

TMIP. It can be concluded that the crystallinity of NIP is higher than that of MIP, and with imprinted sites on the surface of SiO_2, SiO_2/MIP is more amorphous than TMIP.

The results suggest that the amorphous states of MIP could result from imprinting by NC. In other words, compared with pure PMAA, the imprinting process decreases the regularity of the crystalline region in order to make the template molecule orient in the polymer networks. When the polymers are imprinted with SiO_2 as the core material, the amorphous degree of the polymers is at its maximum. This is due to the fact that the polymerization process is severely disorganized when affected by the hydrogen bond interactions among MPS-SiO_2, MAA and NC, which makes the polymerization process deviate greatly from the regular pathway of chain growth of a crystalline polymer, thus leading to the formation of amorphous polymers.

2.5 Thermal properties

The TGA curves of TMIP, TNIP, SiO_2/MIP and SiO_2/NIP in Fig. 6 show scans from 50 °C to 600 °C in an atmosphere of nitrogen. The thermal degradation process of TMIP and SiO_2/MIP consists of four stages. The weight loss of TMIP and SiO_2/MIP at 200 °C is less than 4%, but it increases steeply between 200 °C and 270 °C. This is followed by a sluggish rise from 270 °C to 457 °C and then the curves reach a plateau. In contrast, TNIP and SiO_2/NIP go through three stages with the increase of temperature: TNIP and SiO_2/NIP have a weight loss of nearly 6% at 200 °C and show a straightforward increase in weight loss from 330 °C with a final constant weight at 457 °C.

The 4% weight loss of SiO_2/MIP (and TMIP) and 6% weight loss of SiO_2/NIP (and TNIP) at 200 °C result from adsorbed water. The 50% weight loss of SiO_2/MIP (56% for TMIP) from 200 °C to 270 °C is attributed to the formation of six-membered cyclic intramolecular anhydrides.[35] The sluggish 30% weight loss of SiO_2/MIP (36% for TMIP) from 270 °C to 457 °C derives from degradation to CO_2 and H_2O. The weight loss of SiO_2/NIP (TNIP) from 330 °C is due to the degradation of PMAA.

The residual weights of TMIP, TNIP, SiO_2/MIP and SiO_2/NIP are presented in Table 1.

The results show that SiO_2/NIP (TNIP) is more stable than SiO_2/MIP (TMIP), and that SiO_2/MIP is more stable than TMIP in the same way. This is consistent with the morphology
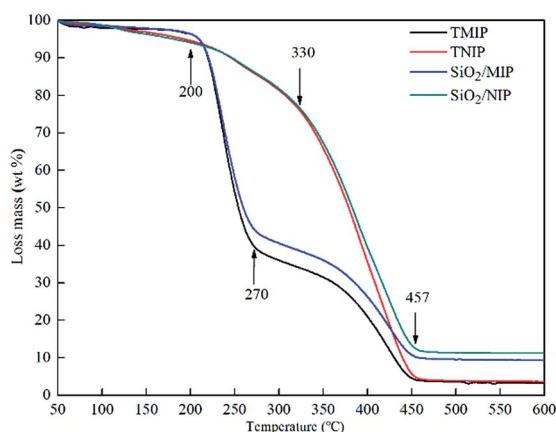
Table 1 The residual weights of the prepared four polymers from their TGA curves

Polymer	Residual weight (%)
TMIP	3.8
TNIP	4.1
SiO_2/MIP	9.7
SiO_2/NIP	11.5

observations of the traditional and surface imprinting polymers. SiO_2/NIP is made up of many bulk agglomerates, therefore, it is more difficult for SiO_2/NIP to transfer the heat when the external temperature is rising, compared with the polyporous polymer networks of SiO_2/MIP, which have lower resistance to heat transmission. It ultimately depends on whether the polymers are imprinted by a template molecule or not. At the same time, SiO_2/MIP is more stable than TMIP, which confirms the successful imprinting on the surface of SiO_2 by NC, and explains the excellent stability of SiO_2 in the trial range of 50–600 °C.

2.6 Adsorption capacity

It is essential to study the adsorption capacity of SiO_2/MIP and SiO_2/NIP for the template NC; this is a critical parameter which can reflect the ability of a material to detect a particular substance. To assess whether surface molecular imprinting technology leads to an excellent adsorption capacity for the template molecule, TMIP and TNIP were compared with SiO_2/MIP and SiO_2/NIP. Fig. 7 explicitly presents the adsorption capacities (Q values) of SiO_2/MIP, SiO_2/NIP, TMIP and TNIP for NC. From the adsorption graph (Fig. 7), it is clear that the Q value of SiO_2/MIP is far above (approximately 21 times) that of SiO_2/NIP. Furthermore, the Q value of TMIP is lower than that of SiO_2/MIP. The Q value of SiO_2/MIP is about 3.5 times the Q value of TMIP. The results show that SiO_2/MIP has an excellent adsorption performance for NC, with a maximum adsorption amount of 1.7 mg mg^{-1} when the concentration of NC is 2 mg ml^{-1}, and through the surface imprinting process, the adsorption capacity is improved effectively.

Fig. 6 TGA traces showing the thermal decomposition of TMIP, TNIP, SiO_2/MIP and SiO_2/NIP in a nitrogen atmosphere.
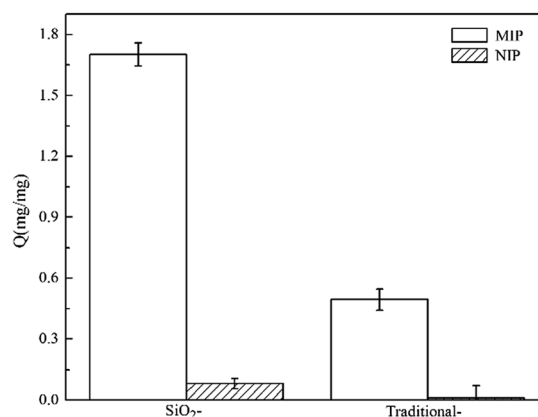

Fig. 7 Adsorption graph of SiO_2/MIP, SiO_2/NIP, TMIP and TNIP.

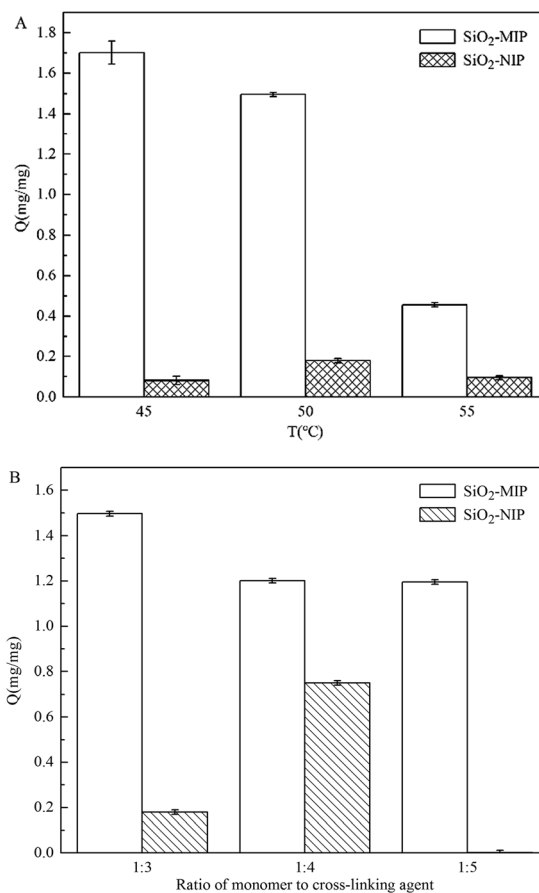## 2.7 Optimization of the polymerization conditions

In order to identify appropriate conditions for the synthesis of SiO$_2$/MIP, the temperature and the proportions of functional monomer and cross-linking agent were studied in this paper. The component proportions and different temperature conditions used in this work are given in Table 2. The adsorption capacities of SiO$_2$/MIP and SiO$_2$/NIP prepared using the different polymerization temperatures and proportions are displayed in Fig. 8.

The polymerization temperature is important for the formation of a polymer network. With a lower external temperature, the polymerization process is difficult to initiate. However, when the temperature is too high, the polymerization advances very quickly, even developing into an implosion. The proportions of the functional monomer and cross-linking agent are another important parameter. A lower amount of cross-linking agent is beneficial for increasing the cross-linking index of the final polymers and speeding up the process of polymerization. However, excessive cross-linking agent can result in the formation of a rigid polymer, which is detrimental to the adsorption capacity for NC.

In consideration of the explosion hazard of NC at higher temperatures and the reactive ability of MAA at low temperatures, the temperatures of 45 °C, 50 °C and 55 °C were chosen for polymerization. As shown in Fig. 8(A), when the polymerization temperature was controlled at 45 °C, the resulting SiO$_2$/MIP realized the best adsorption performance. With a temperature of 45 °C, the Q value of SiO$_2$/MIP was 20.9 times that of SiO$_2$/NIP, 1.2 times that of SiO$_2$/MIP prepared at 50 °C, and 3.7 times that of SiO$_2$/MIP prepared at 55 °C. This indicates that the polymerization is exactly initiated at the temperature of 45 °C. The decomposition of the initiator is an endothermal reaction, and the decomposition rate of AIBN is slow. When the temperature is increased, more free radicals can be produced by AIBN. Plenty of free radicals attack the monomers and accelerate the process of chain propagation. Chain propagation is an exothermic process. So at higher temperatures, the reaction balance deviates to the depolymerization processes, which results in the formation of a polymer with a low polymerization degree. The polymer networks of SiO$_2$/MIP with a low polymerization degree are loose and cannot immobilize NC molecules sufficiently. However, the SiO$_2$/MIP prepared at 45 °C has the appropriate cross-linking network density to fix more NC

Fig. 8 Influence of polymerization temperature (A) and the ratio of monomer to cross-linker (B) for SiO$_2$/MIP and SiO$_2$/NIP on the adsorption of NC.

molecules, and is not too rigid to hinder the access of NC to the imprinted sites during the recombination process. The results show that increasing the temperature is favorable for the polymerization process, but it is adverse to the adsorption of NC.

From the adsorption capacities graph of SiO$_2$/MIP with different proportions of functional monomer and cross-linking agent (Fig. 8(B)), the SiO$_2$/MIP prepared with the ratio of 1 : 3 has the best adsorption capacity and specificity, while with the ratio of 1 : 4, the specificity of SiO$_2$/MIP is inferior. The adsorption capacity of SiO$_2$/MIP for NC is 8.3 times and 857 times that of SiO$_2$/NIP, when prepared with ratios of 1 : 3 and 1 : 5, respectively, while the adsorption capacity of SiO$_2$/MIP is 1.6 times that of SiO$_2$/NIP when prepared with a ratio of 1 : 4. It is concluded that the maximum adsorption capacities can be reached when the temperature is 45 °C and the ratio of functional monomer to cross-linking agent is 1 : 3.

2.8 Selectivity of SiO$_2$/MIP

The structures of NC and its analogues are shown in Fig. 9. NC, and its analogues methyl cellulose (MC), carboxymethyl cellulose (CMC) and hydroxypropyl cellulose (HPC), are derivatives of cellulose, which are formed through substitution reactions of hydroxyl groups with nitric ester, methoxyl, carboxymethyl and

Table 2 Effects of temperature and proportion on adsorption capacity to NC

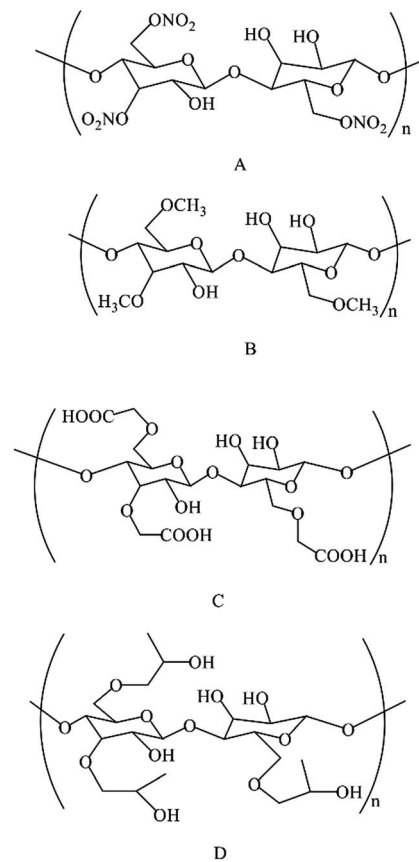| Variate	NC (g)	MAA (mmol)	EGDMA (mmol)	MPS-SiO$_2$ (g)	AIBN (g)	Acetone (ml)	T (°C)
T	0.1	3	9	0.1	0.1642	30	45
							50
							55
Proportion	0.1	3	9	0.1	0.1642	30	50
			12				
			15				

Fig. 9 Structures of NC (A) and its analogues: MC (B), CMC (C) and HPC (D).

hydroxypropyl groups, respectively. The SiO_2/MIP and SiO_2/NIP were prepared with a polymerization temperature of 45 °C and a ratio of monomer to cross-linking agent of 1 : 3. The adsorption capacities of SiO_2/MIP and SiO_2/NIP particles for the three analogues of NC in aqueous solutions are shown in Fig. 10. Meanwhile, the corresponding UV-vis spectra and standard curves are depicted in Fig. 11. In comparison with SiO_2/NIP, it is obvious that SiO_2/MIP possesses higher adsorption capacities for the analogues of NC. This results from the fact that the
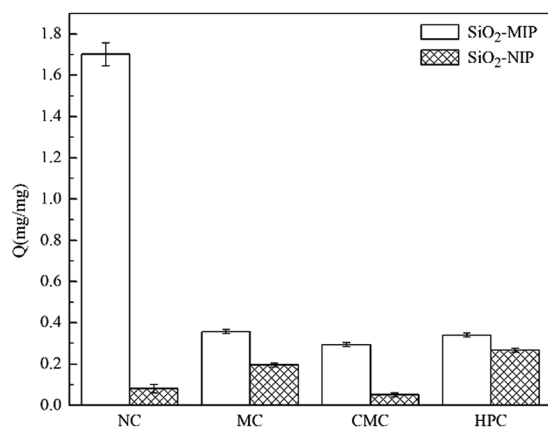

Fig. 10 Binding amounts of different cellulose derivatives.
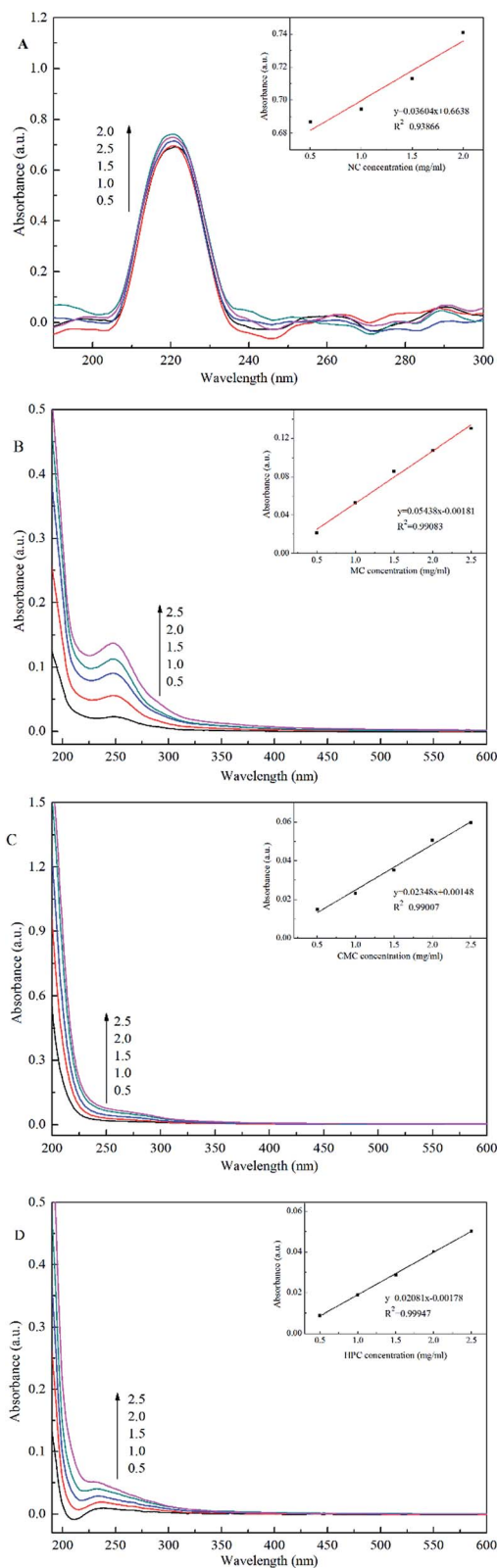

Fig. 11 UV-vis spectra of NC (A) and its analogues: MC (B), CMC (C), and HPC (D). The insets show the standard curves for each substance. The solvent for NC in this work was acetone; deionized water was used as the solvent for the other analogues, without any exception.

imprinting cavities and bigger surface area inside the SiO$_2$/MIP make it easier for it to combine with analogues of NC, while no imprinting sites are available inside the SiO$_2$/NIP. However, the adsorption capacities of SiO$_2$/MIP towards MC, CMC and HPC are very weak. The adsorption capacity of SiO$_2$/MIP for NC is approaching 5 times more than that for CMC, which can be ascribed to the unsuitable imprinting cavities inside SiO$_2$/MIP for MC, CMC and HPC in terms of shape, size, and functional distribution. The results confirm the particular selectivity of SiO$_2$/MIP for NC.

3. Conclusions

This paper introduces a novel detection method for NC using surface molecularly imprinted technology. The synthesized SiO$_2$/MIP consists of a polyporous and amorphous polymer matrix on the surface of SiO$_2$ particles. Through FT-IR analysis, the removal of NC is shown to be thorough; there is no residual NC in imprinted materials. The thermal analysis and study of crystalline states confirm the successful imprinting of NC in the polymers. The prepared SiO$_2$/MIP exhibits a high adsorption capacity and an excellent selectivity for NC, which opens a new pathway for the detection of NC. This method could also be applied to the detection of other flammable explosives. The SiO$_2$/MIP material could be further used in security checks and contaminant adsorption.

4. Experimental

4.1 Reagents and materials

Nitrocellulose (NC, A grade) was provided by North Sichuan Nitrocellulose Co., China. 2,2-Azobisisobutyronitrile (AIBN, 98.5%), 3-(trimethoxysilyl) propylmethacrylate (MPS, 97%), ethanol (99.7%), acetic acid (99.5%) and deionized water were purchased from Nanjing Chemical Reagent Co., Nanjing, China. Methylacrylic acid (MAA, 98%), tetraethoxysilicane (TEOS), acetone (99.7%) and methanol (99.5%) were obtained from Sinopharm Chemical Reagent Co., Nanjing, China. Ammonium hydroxide was provided by Shanghai Lingfeng Chemical Reagent Co., China. Ethylene glycol dimethacrylate (EGDMA, 98%) was purchased from Aladdin Reagent Co., Shanghai, China. Methyl cellulose (MC, 15 mPa s) was purchased from Meryer Chemical Technology Co., Shanghai, China. Carboxymethyl cellulose (CMC, 600–1000 mPa s, USP grade) and hydroxypropyl cellulose (HPC, M. W.100 000) were purchased from Macklin Biochemical Co., Shanghai, China. AIBN was recrystallized from ethanol before use, and all other chemicals were used directly without purification.

4.2 Surface pre-treatment of SiO$_2$ particles

SiO$_2$ particles were prepared according to the previously reported method.[23] Then MPS was used to improve the affinity of the SiO$_2$ particles for NC. Briefly, SiO$_2$ particles (0.5 g), deionized water (5 ml), aqueous ammonia (6 ml), and MPS (3 ml) were ultrasonically dispersed in ethanol (50 ml) for 1 h.[36] Then the mixture was transferred into a 150 ml round-bottom flask and stirred at 75 °C in a dry nitrogen atmosphere for 4 h. After the reaction, the

products were centrifuged and washed with ethanol three times to remove the unreacted MPS. Finally, the resultant MPS-SiO$_2$ particles were obtained after a vacuum drying procedure.

4.3 Preparation of SiO$_2$/MIP

SiO$_2$/MIP particles were prepared through in situ polymerization in which MAA was used as a functional monomer and EGDMA was used as a cross-linking agent. Briefly, NC (0.1 g) was dissolved in acetone (30 ml) and then MAA (3 mmol), EGDMA (9 mmol), and MPS-SiO$_2$ particles (0.1 g) were dispersed in the NC solution by ultrasonication for 10 min. Subsequently, AIBN (0.1642 g) was added and the above solution was transferred to a 150 ml round-bottom flask to react at 50 °C with continuous stirring in a dry nitrogen atmosphere for about 4 h. Finally, the polymers were added to methanol/acetic acid (4 : 1, v/v) solution with ultrasonication for 2 h to remove the NC. The resultant SiO$_2$/MIP particles were obtained by vacuum drying after washing with ethanol and deionized water and centrifuging three times to remove residual methanol and acetic acid. As a control, the corresponding SiO$_2$/NIP was synthesized using an identical method but without the addition of NC.

4.4 Preparation of TMIP

TMIP particles were synthesized for comparison; the preparation procedure was as follows: NC (0.1 g) was dissolved in acetone (30 ml). MAA (3 mmol) and EGDMA (9 mmol) were added to the solution above following ultrasonication for 10 min. Subsequently, AIBN (0.1642 g) was added, the mixture was transferred to a 150 ml round-bottom flask and the reaction was processed at 50 °C with continuous stirring in a dry nitrogen atmosphere for about 4 h. After the final removal of NC and vacuum drying, the resultant TMIP particles were obtained.

The TNIP particles were synthesized using the same method but in the absence of the NC template.

4.5 Adsorption capacities of SiO$_2$/MIP and SiO$_2$/NIP

Adsorption capacities were studied using the following procedures: 10 mg SiO$_2$/MIP (SiO$_2$/NIP, TMIP or TNIP) were added into a 10 ml 2 mg ml^{-1} NC solution. After ultrasonication for 2 h, the supernatant liquid was collected through centrifugation. The concentration of supernatant liquid was measured by UV-vis spectrophotometry. The NC amount bound by SiO$_2$/MIP was calculated by the following equation:

$$Q = (c_0 - c_e)V/m \qquad (1)$$

where, Q (mg mg^{-1}) is the NC amount bound by SiO$_2$/MIP (SiO$_2$/NIP, TMIP or TNIP), c_0 (mg ml^{-1}) is the initial concentration of NC, c_e (mg ml^{-1}) is the concentration of the supernatant liquid, V (ml) is the volume of NC solution, m (mg) is the mass of SiO$_2$/MIP (SiO$_2$/NIP, TMIP or TNIP).

4.6 Effects of polymerization conditions on adsorption capacity

To evaluate the effects of polymerization temperature and the proportions of functional monomer and cross-linking agent on

the adsorption capacity of SiO$_2$/MIP, the polymerization process was conducted at different temperatures and monomer to cross-linking ratios.

Temperature: NC (0.1 g) was dissolved in acetone (30 ml) and then MAA (3 mmol), EGDMA (9 mmol), and MPS-SiO$_2$ particles (0.1 g) were dispersed in the NC solution by ultrasonication for 10 min. Subsequently, AIBN (0.1642 g) was added, the mixture was transferred to a 150 ml round-bottom flask and the reaction was processed at either 45 °C or 55 °C with continuous stirring in a dry nitrogen atmosphere for 4 h. After the final removal of NC and vacuum drying, the resultant MIP particles were obtained. The amount of bound NC was calculated according to eqn (1).

Proportions: NC (0.1 g) was dissolved in acetone (30 ml) and then MAA (3 mmol), EGDMA (12 mmol or 15 mmol), and MPS-SiO$_2$ particles (0.1 g) were dispersed in NC solution by ultrasonication for 10 min. Subsequently, AIBN (0.1642 g) was added, the mixture was transferred to a 150 ml round-bottom flask and the reaction was processed at 50 °C with continuous stirring in a dry nitrogen atmosphere for 4 h. After the final removal of NC and vacuum drying, the resultant MIP particles were obtained. The amount of bound NC was calculated according to eqn (1).

4.7 Selectivity performance of SiO$_2$/MIP and SiO$_2$/NIP

20 mg MC (CMC or HPC) were dissolved into 10 ml deionized water, after the addition of 10 mg SiO$_2$/MIP (or SiO$_2$/NIP). After ultrasonication for 2 h, the supernatant liquid was obtained by centrifugation. The concentration of MC (CMC or HPC) in the supernatant liquid was measured by UV-vis spectrophotometry. The amount of bound MC (CMC or HPC) was calculated according to eqn (1).

4.8 Characterization

The functional groups of pure SiO$_2$, MPS-SiO$_2$, SiO$_2$/MIP, SiO$_2$/NIP and NC were confirmed by Fourier transform infrared (FT-IR, Nicolet iS10, America) spectroscopy in the range of 4000–500 cm^{-1}. The morphological structures of SiO$_2$/MIP particles were obtained from scanning electron microscopy (SEM, FEG-250, Quanta, America, operating at 40 kV). The crystalline states of SiO$_2$ and SiO$_2$/MIP were determined through X-ray diffraction (XRD, D8 Advance, Germany) with conditions as follows: Cu Kα radiation ($\lambda = 1.5406$), 40 kV, 40 mA, 2θ scanning range of 10–90°, step size of 0.05° and step time of 19.2 s. The thermogravimetric analysis (TGA) was performed on a SDTQ600 thermal analyzer (PerkinElmer Pyris Diamond, America) under a nitrogen atmosphere at a heating rate of 10 °C min^{-1}. The adsorption capacity of SiO$_2$/MIP particles was analyzed by ultraviolet-visible (UV-vis) spectrophotometry (Evolution 220, America).

Conflicts of interest

There are no conflicts to declare.

References

1 W. Tomaszewski, K. Cieślak and A. Zygmunt, *Polym. Degrad. Stab.*, 2015, **111**, 169–175.
2 X. Su, Q. Zhao, D. Zhang and W. Dong, *Appl. Surf. Sci.*, 2015, **356**, 610–614.
3 Z. Xiao, S. Ying, W. He, F. Xu and P. Sun, *J. Appl. Polym. Sci.*, 2007, **105**, 510–514.
4 L.-T. Yin, Y.-T. Lin, Y.-C. Leu and C.-Y. Hu, *Sens. Actuators, B*, 2010, **148**, 207–213.
5 M. Cretich, V. Sedini, F. Damin, M. Pelliccia, L. Sola and M. Chiari, *Anal. Biochem.*, 2010, **397**, 84–88.
6 L. Hecht, D. van Rossum and A. Dietzel, *Microelectron. Eng.*, 2016, **158**, 52–58.
7 S. Ma, G. Song and N. Feng, *Carbohydr. Polym.*, 2012, **89**, 36–40.
8 A. S. Chajistamatiou and E. B. Bakeas, *Talanta*, 2016, **151**, 192–201.
9 D. K. MacMillan, C. R. Majerus, R. D. Laubscher and J. P. Shannon, *Talanta*, 2008, **74**, 1026–1031.
10 H. Rao, M. Chen, H. Ge, Z. Lu, X. Liu, P. Zou, X. Wang, H. He, X. Zeng and Y. Wang, *Biosens. Bioelectron.*, 2017, **87**, 1029–1035.
11 M. Huang, T. Zhou, X. Wu and J. Mao, *Chin. J. Chem. Eng.*, 2015, **23**, 1698–1704.
12 Z. F. Cai, H. J. Dai, S. H. Si and F. L. Ren, *Appl. Surf. Sci.*, 2008, **254**, 4457–4461.
13 G. Erturk and B. Mattiasson, *J. Chromatogr. B: Anal. Technol. Biomed. Life Sci.*, 2016, **1021**, 30–44.
14 M. Perez, R. Concu, M. Ornelas, M. N. Cordeiro, M. Azenha and A. F. Silva, *Spectrochim. Acta, Part A*, 2016, **153**, 661–668.
15 J. Li, S. M. Li and Z. G. He, *Mater. Sci. Eng., C*, 2017, **71**, 999–1003.
16 A. Sorribes-Soriano, F. A. Esteve-Turrillas, S. Armenta, M. de la Guardia and J. M. Herrero-Martinez, *J. Chromatogr. A*, 2017, **1481**, 23–30.
17 Y. Zhang, J. Wan and X. Cao, *Process Biochem.*, 2016, **51**, 517–527.
18 C. K. M. Faizal and T. Kobayashi, *Polym. Eng. Sci.*, 2008, **48**, 1085–1093.
19 B. R. Hart and K. J. Shea, *Macromolecules*, 2002, **35**, 6192–6201.
20 D. Oliveira, C. P. Gomes, R. C. S. Dias and M. R. P. F. N. Costa, *React. Funct. Polym.*, 2016, **107**, 35–45.
21 C. Baggiani, C. Giovannoli, L. Anfossi, C. Passini, P. Baravalle and G. Giraudi, *J. Am. Chem. Soc.*, 2012, **134**, 1513–1518.
22 M. Torkashvand, M. B. Gholivand and G. Malekzadeh, *Sens. Actuators, B*, 2016, **231**, 759–767.
23 R. Gao, J. Zhang, X. He, L. Chen and Y. Zhang, *Anal. Bioanal. Chem.*, 2010, **398**, 451–461.

24 A. M. Shrivastav, S. P. Usha and B. D. Gupta, *Biosens. Bioelectron.*, 2016, **79**, 150–157.

25 W. Tan, Q. Yu, X. Ruan and X. Huang, *Sens. Actuators, B*, 2015, **212**, 47–54.

26 H. Duan, X. Wang, Y. Wang, J. Li, Y. Sun and C. Luo, *Sens. Actuators, B*, 2016, **236**, 44–51.

27 Y. Liu, B. Cao, P. Jia, J. An, C. Luo, L. Ma, J. Chang and K. Pan, *J. Phys. Chem. A*, 2015, **119**, 6661–6667.

28 B. Yuan, X. Q. Yang, L. W. Xue, Y. N. Feng and J. H. Jiang, *Bioresour. Technol.*, 2016, **222**, 14–23.

29 H. Duan, X. Wang, Y. Wang, Y. Sun, J. Li and C. Luo, *Anal. Chim. Acta*, 2016, **918**, 89–96.

30 Z. Wang and X. Cao, *Process Biochem.*, 2015, **50**, 1136–1145.

31 C. G. Xie, B. H. Liu, Z. Y. Wang, D. M. Gao, G. J. Guan and Z. P. Zhang, *Anal. Chem.*, 2008, **80**, 437–443.

32 N. Sun, X. Meng and Z. Xiao, *Ceram. Int.*, 2015, **41**, 13830–13835.

33 Z. Xiao, P. Guo and N. Sun, *J. Appl. Polym. Sci.*, 2017, **134**, 44377.

34 N. Bogdanchikova, A. Pestryakov, M. H. Farias, J. A. Diaz, M. Avalos and J. Navarrete, *Solid State Sci.*, 2008, **10**, 908–914.

35 A. Asano and T. Kurotu, *Polym. Degrad. Stab.*, 2002, **78**, 137–141.

36 X. Wang, J. Yu, Q. Kang, D. Shen, J. Li and L. Chen, *Biosens. Bioelectron.*, 2016, **77**, 624–630.